HHS Public Access

Author manuscript

Atherosclerosis. Author manuscript; available in PMC 2017 February 01.

Published in final edited form as:

Atherosclerosis. 2016 August ; 251: 109–118. doi:10.1016/j.atherosclerosis.2016.06.011.

A single injection of gain-of-function mutant PCSK9 adeno-associated virus vector induces cardiovascular calcification in mice with no genetic modification

Claudia Goettsch[1,*], **Joshua D. Hutcheson**[1,*], **Sumihiko Hagita**[1,*], **Maximillian A. Rogers**[1], **Michael D. Creager**[1], **Tan Pham**[1], **Jung Choi**[1], **Andrew K Mlynarchik**[1], **Brett Pieper**[1], **Mads Kjolby**[3], **Masanori Aikawa**[1,2], and **Elena Aikawa**[1,2]

[1]Center for Interdisciplinary Cardiovascular Sciences, Cardiovascular Division, Brigham and Women's Hospital, Harvard Medical School, Boston, MA, 02115, USA

[2]Center for Excellence in Vascular Biology, Cardiovascular Division, Brigham and Women's Hospital, Harvard Medical School, Boston, MA, 02115, USA

[3]The Lundbeck Foundation Research Center MIND and The Danish Research Institute of Translational Neuroscience, Nordic EMBL Partnership for Molecular Medicine, and Danish Diabetes Academy, Department of Biomedicine, Aarhus University, 8000, Denmark

Abstract

Background—Studying atherosclerotic calcification *in vivo* requires mouse models with genetic modifications. Previous studies showed that injection of recombinant adeno-associated virus vector (AAV) encoding a gain-of-function mutant PCSK9 into mice promotes atherosclerosis.

Aim—We aim to study cardiovascular calcification induced by PCSK9 AAV in C57BL/6J mice.

Methods—10 week-old C57BL/6J mice received a single injection of AAV encoding mutant mPCSK9 (rAAV8/D377Y-mPCSK9). *Ldlr*$^{-/-}$ mice served as positive controls. Mice consumed a high-fat, high-cholesterol diet for 15 or 20 weeks. Aortic calcification was assessed by fluorescence reflectance imaging (FRI) of a near-infrared calcium tracer.

Results—Serum levels of PCSK9 (0.14 μg/ml to 20 μg/ml, $p < 0.01$) and total cholesterol (82 mg/dL to 820 mg/dL, $p < 0.01$) increased within one week after injection and remained elevated for 20 weeks. Atherosclerotic lesion size was similar between PCSK9 AAV and *Ldlr*$^{-/-}$ mice. Aortic calcification was 0.01%±0.01 in PCSK9 AAV mice and 15.3%±6.1 in *Ldlr*$^{-/-}$ mice at 15 weeks ($p < 0.01$); by 20 weeks, the PCSK9 AAV mice aortic calcification grew to 12.4%±4.9. Tissue non-specific alkaline phosphatase activity was similar in PCSK9 AAV mice and *Ldlr*$^{-/-}$ mice at 15 and 20 weeks, respectively. As example of the utility of this model in testing modulators of calcification *in vivo*, PCSK9 AAV injection to sortilin-deficient mice demonstrated reduced aortic calcification by 46.3% ($p < 0.05$) compared to littermate controls.

Correspondence to Elena Aikawa, MD, PhD, Center for Interdisciplinary Cardiovascular Sciences, 3 Blackfan Circle, CLS, 17th floor, Boston, MA 02115, Phone: 617-730-7700; Fax: 617-730-7791, eaikawa@partners.org.

*Equal contribution

Conflict of interest statement

SH is an employee of KOWA Company, Ltd., Nagoya, Japan. Other authors have no conflict of interest.

Conclusion—A single injection of gain-of-function PCSK9 AAV into C57BL/6J mice is a useful tool to study cardiovascular calcification in mice with no genetic manipulation.

Keywords

cardiovascular calcification; AAV-PCSK9; animal model

Introduction

Cardiovascular calcification correlates with age and cardiovascular risk factors. Calcification in atheromata reduces plaque integrity and can enhance risk of rupture and subsequent acute myocardial infarction. Atherosclerotic calcification, particularly when presented as low-density microcalcifications in the fibrous cap, predicts cardiovascular events [1–3]. Clinical imaging studies identified spotty calcification as a marker of plaques prone to acute coronary syndrome [4]. Moreover, computational modeling indicated that microcalcification increases stress concentrations at the surface of thin-capped atheroma implicated in plaque rupture [5, 6]. Although ectopic calcification causes serious devastating clinical problems, no medical therapies have been established.

In vivo validation of novel targets for the contribution of a protein to intimal calcification requires the development of genetically deficient animals - a costly and time-consuming process. It commonly takes approximately two years to generate colonies of sufficient size [7]. Within the cardiovascular field - genetic engineering is typically performed by crossbreeding C57BL/6 mice with mice deficient in low-density lipoprotein receptor (*Ldlr*) or apolipoprotein E (*Apoe*), because wild-type C57BL/6 do not develop atherosclerotic calcification. To study intimal calcification, a 15 to 20 week feeding period with a diet high in fat and cholesterol is subsequently necessary [8, 9]. Accelerating the pace of target validation in the field of vascular calcification by avoiding cross-breeding to atherosclerotic mice strains would greatly enhance research efficiency.

Recent studies showed that a single injection of a recombinant adeno-associated virus vector (AAV) encoding a gain-of-function mutant form of proprotein convertase subtilisin/kexin type 9 (PCSK9) in combination with an atherogenic diet for up to 24 weeks induces atherosclerosis in mice and hamsters [10, 11]. PCSK9 transgenic mice [12] and D374Y-PCSK9 transgenic pigs [13, 14] develop atherosclerotic lesions with the features of calcification. PCSK9 levels predict cardiovascular events in patients with stable coronary heart disease [15].

We therefore hypothesized that a single injection of a recombinant AAV encoding a gain-of-function mutant form of PCSK9 helps to avoid genetic manipulations to study cardiovascular calcification in C57BL/6J mice.

Material and Methods

Animal procedures

C57BL/6J mice (cat#000664) and LDL receptor deficient mice (*Ldlr*$^{-/-}$, B6.129S7-Ldlrtm1Her/J, cat#002207) were purchased from Jackson Laboratory (Bar Harbor, ME,

USA) and bred at the Beth Israel Deconess Medical Center animal facility. *Sort*$^{-/-}$ mice were generated by targeted deletion of 191 bp of exon 14 (genOway) as described previously [9]. *Sort*$^{+/+}$ littermate were used as controls. Male and female C57BL/6J (*Sort*$^{+/+}$), *Sort*$^{-/-}$ mice and *Ldlr*$^{-/-}$ mice were used in all experiments. The recombinant murine PCSK9 adeno-associated virus (pAAV/D377Y-mPCSK9) was produced at the Gene Therapy Center Vector Core at The University of North Carolina (Chapel Hill, NC, USA) using the PCSK9 gain-of-function plasmid [10]. To deliver AAV, 10 week-old mice were given 10^{11} vector genome copies of pAAV/D377Y-mPCSK9 (PCSK9 AAV) [10] or saline control via single tail vein injection (Figure 1A). Thereafter, mice were fed a high-fat, high-cholesterol (HF/HC) diet (21% fat and 1.25% cholesterol, Research Diets D12108C, New Brunswick, NJ, USA) for 15 or 20 weeks. Two mice were fed for 30 weeks. Age- and gender matched *Ldlr*$^{-/-}$ mice that consumed the same diet for 15 or 20 weeks served as controls.

Blood was collected from (submandibular) facial vein before, and 1, 2, 5, 10, 15 and 20 weeks after AAV injection and stored at −80°C until further use. For histology, aortic roots and arches were embedded in OCT compound and stored at −80°C until use.

All animal experiments were approved by and performed in compliance with the Institutional Animal Care and Use Committee at Beth Israel Deaconess Medical Center under animal protocol #010–2013 (Boston, MA, USA).

Macroscopic Fluorescence Reflection Imaging

Calcification in the aorta was monitored *ex vivo* as described previously [8]. A bisphosphonate-conjugated near-infrared fluorescent (NIRF) imaging agent (Osteosense-680 EX, PerkinElmer, Boston, MA, USA) was intravenously administered via tail vein into the mice 24 hours before imaging. After mice were euthanized, the aorta was perfused with saline through the posterior end of left ventricle using 25G needle and syringe, dissected and imaged to map the macroscopic NIRF signals elaborated by Osteosense680 (excitation/emission: 668±10/687±10nm) using fluorescent reflection imaging (FRI, Image Station 4000MM, Eastman Kodak Co., New Haven, CT, USA). The FRI was performed using excitation/emission filter sets of 630nm/700 nm with an f-stop setting of 2.4, the field of view set to 83.96 mm, the focal plane set at 7.61 mm, and an exposure time of 180 sec. After image acquisition, a custom MATLAB script was used to calculate the NIRF-positive regions (Supplemental Methods). The Bio-Formats Open Microscopy Library platform was used to import the raw FRI data into MATLAB. The images were converted to a 16bit format, and a region of interest (a 200 pixel × 200 pixel region containing the aortic arch and root) was drawn to select the aortic arch and roots of each within each specimen. Thresholds were set such that a pixel intensity of 4.5×10^4 was considered NIRF-positive and were kept constant for all mice analyzed. Positive pixels were then divided by the total area to determine the NIRF-positive fraction.

Blood measurements

Plasma concentrations of PCSK9, dickkopf-1 (Dkk1) and osteoprotegerin (OPG) were determined using ELISA Kits from R&D systems (Minneapolis, MN, USA). Plasma total cholesterol and triglyceride levels were assessed using a kit from Wako Pure Chemical

Industries (Osaka, Japan; Cholesterol E-test, Triglyceride E-test). Plasma levels of calcium and phosphate were measured using kits from BioVision (Milpitas, CA, USA) and BioAssay Systems (Hayward, CA, USA).

Histology and image quantification

Tissue samples were frozen in OCT compound and 7 μm serial sections were cut and stained with hematoxylin and eosin for overall morphology. Lipids were detected with Oil Red O staining. Tissue non-specific alkaline phosphatase activity (an early marker of osteoblastic activity) was detected on unfixed cryosections according to manufacturer instructions (Vector Labs, Burlingame, CA, USA). For von Kossa silver stain for inorganic phosphate calcium salts, sections were incubated with 5% silver nitrate (American Master Tech Scientific, Lodi, CA, USA) for 60 min under UV light, then washed with sodium thiosulfate. Nuclei were stained with nuclear fast red (American Master Tech Scientific, Lodi, CA, USA). Fibrillar collagen in the plaques was identified by picrosirius red staining and captured by polarized microscopy. When visualized under polarized light, picrosirius red exhibits birefringence that distinguishes mature, or thick collagen bundles (yellow-orange hue) from immature or disrupted thin collagen fibers (green hue) [16]. Slides were examined using Eclipse 80i microscope (Nikon, Melville, NY, USA). Image quantification was performed with Elements 3.20 software (Nikon).

Immunohistochemistry/Immunofluorescence

Tissue samples were cut into 7-μm thin slices histological sections, and cryo-sections were fixed in acetone. After blocking in 4% serum, sections were incubated with fluorescently-labeled primary antibodies (mouse α-smooth muscle cell actin-Cy3 [1:500, Dako, Carpinteria, CA, USA]; and mouse CD68-Alexa Fluor 488 [1:100, Novus, Littleton, CO, USA]). Sections were washed in PBS and embedded in a mounting medium containing DAPI (Vector Laboratories). Slides were examined using a confocal microscope (Nikon A1).

For bright field immunohistochemistry on tissue sections, after blocking in 4% serum, sections were incubated with an antibody against mouse sortilin [AF2934, 1:20; R&D Systems, Minneapolis, MN, USA], Runx2 [M-70, 1:20, Santa Cruz, Dallas, TX, USA], and or osteocalcin [ab93876, 1:20, Abcam, Boston, MA, USA], followed by incubation with a biotin-labeled secondary antibody. Sections were then incubated with streptavidin-labeled HRP solution (Dako, Carpinteria, CA, USA), followed by an AEC solution (Dako, Carpinteria, CA, USA). Slides were examined using an Eclipse 80i microscope (Nikon, Melville, NY, USA). All images were processed with Elements 3.20 software (Nikon).

Preparation of liver homogenates and western blotting

Liver homogenates were prepared in RIPA buffer (Thermo Scientific, Cambridge, MA, USA) containing protease and phosphatase inhibitors. Briefly, a portion of mouse liver tissue was homogenized in an ice cold 1.5mL tube with a disposable plastic pestle using ice cold RIPA buffer containing freshly dissolved protease and phosphatase inhibitor pellets. Samples were run through a syringe and then centrifuged at 12,000g for 5 minutes at 4 degrees C. Supernatants were collected and run through a 27G1/2 syringe (Becton Dickinson and Company, Franklin Lake, NJ, USA) five times. Protein was quantified using

the BCA assay (Thermo Scientific, Cambridge, MA, USA), and 100ug of protein in SDS sample loading buffer (Boston Bioproducts, Ashland, MA, USA) was loaded onto a 10% SDS-PAGE gel. Gels were transferred onto nitrocellulose membranes, blocked in 5% milk for one hour at room temperature, and incubated overnight at 4 degrees C in primary antibody (1:1000 LDL receptor (LDLR) antibody BioVision Inc, Milpitas, CA, USA, cat#3839-100; 1:1000 LDLR-related protein 1 (LRP1) antibody Abcam, Boston, MA, USA, cat#92544; 1:200 VLDLR antibody Santa Cruz Biotechnology, Dallas, TX, USA, cat#sc-18824; 1:5000 beta-actin antibody Novus, Littleton, CO, USA, cat#NB600-501). After washing the membranes five times in TBST (5 minutes per wash at room temperature) they were incubated in corresponding secondary antibodies (1:5000 anti-mouse and anti-rabbit; GE Healthcare) at room temperature for one hour. Membranes were then washed an additional five times in TBST and incubated with a 1:1 mixture of SuperSignal substrate (Thermo Scientific, Cambridge, MA, USA), followed by immediately imaging the membranes using an Image Quant LAS 4000 (GE, Marlborough, MA, USA).

Statistical analysis

Data are given as mean ± SD; n indicates the number of mice. Statistical analyses were performed using GraphPad Prism Version 5 (Prism Software, Inc., La Jolla, CA, USA). For comparison between two groups, a paired or unpaired two-tail Student's *t* test with equal or unequal variances was performed. For comparison among three or more treatment groups, one-way ANOVA followed by Bonferroni's post hoc test was done. Exclusion criteria were set by Grubbs test. No statistical method was used to predetermine sample size. The quantitative analyses for histology were performed blinded to allocation during outcome assessment. Tests with a *P* value less than 0.05 were considered statistically significant.

Results

A single injection of mutant mPCSK9 (D377Y) AAV increased serum cholesterol and atherosclerotic lesions in wild-type C57BL/6J mice

One week after a single PCSK9 AAV injection and being placed on a HF/HC diet, plasma PCSK9 levels of wild-type C57BL/6J mice increased from 0.13 ± 0.04 μg/ml to 19.4 ± 11.7 μg/ml ($p < 0.0001$) and plateaued at this level for 20 weeks (Figure 1B). Saline control mice that consumed a HF/HC diet for 20 weeks had no change in PCSK9 levels (0 wk: 0.138 ± 0.023 μg/ml; 10 wk: 0.136 ± 0.059 μg/ml; 20 wk: 0.204 ± 0.119 μg/ml, $p=0.52$). PCSK9 AAV injection did not alter body weight (Figure 1C).

A single PCSK9 AAV injection and a HF/HC diet for 15 weeks decreased LDLR protein levels in the liver compared to saline control mice ($p < 0.0001$) (Figure 1D), while LRP1 and VLDLR protein levels did not change.

Total cholesterol levels increased one week after a single PCSK9 AAV injection and HF/HC diet from 81 ± 14 mg/dL to 706 ± 126 mg/dL ($p < 0.0001$). In $Ldlr^{-/-}$ mice, one week of HF/HC diet increased total cholesterol levels from 238 ± 47 mg/dL to 980 ± 135 mg/dL ($p < 0.0001$) (Figure 1E). Total cholesterol levels in the PCSK9 AAV group increased to similar levels of those of $Ldlr^{-/-}$ over the 20 weeks of HF/HC diet. Mice consuming a HF/HC diet

for 30 weeks (n=2) after PCSK9 AAV injection retained elevated plasma PCSK9 and total cholesterol (Supplementary Figure 1A, B).

Mice that received PCSK9 AAV and the HF/HC diet for 15 and 20 weeks developed atherosclerotic lesions at the aortic sinus similar in size to *Ldlr*$^{-/-}$ mice (Figure 2A-C). At the lesser curvature, the PCSK9 AAV mice that consumed the HF/HC diet for 20 weeks had significant smaller lesions compared to *Ldlr*$^{-/-}$ mice (Figure 2A, B, D). Saline control mice that consumed the HF/HC diet for 20 weeks did not develop atherosclerotic lesions (Figure 2A-D). PCSK9 AAV injection and the HF/HC diet for 15 or 20 weeks caused aortic valve leaflet thickening similar to that seen in the *Ldlr*$^{-/-}$ mice (Figure 2A, E).

Mutant mPCSK9 (D377Y) AAV injection induces vascular calcification in wild-type C57BL/6J mice

We then assessed the effects of a single PCSK9 AAV injection and HF/HC diet on vascular calcification in wild-type C57BL/6J mice. *Ldlr*$^{-/-}$ mice consuming the HF/HC diet served as positive controls.

Fluorescence reflectance imaging (FRI) of the NIRF calcium tracer in intact arteries detected vascular calcification in all 8 PCSK9 AAV mice on the HF/HC diet for 20 weeks (12.4 ± 4.9 %) (Figure 3A, B). The calcification area was similar to that in *Ldlr*$^{-/-}$ mice on the HF/HC diet for 15 weeks (15.3 ± 6.1 %). *Ldlr*$^{-/-}$ mice that consumed the HF/HC diet for 20 weeks developed more calcification (31.6 ± 4.1 %) compared to the 15 week group and the PCSK9 AAV group. Wild-type C57BL/6J mice that consumed the HF/HC diet for 30 weeks (n=2) after PCSK9 AAV injection had 46.3% and 45.5% calcification area (Supplementary Figure 1C).

Mice that received a single PCSK9 AAV injection and the HF/HC diet for 15 and 20 weeks revealed alkaline phosphatase activity (TNAP-positive lesions) at the aortic sinus, lesser curvature and valve leaflets at the similar level to *Ldlr*$^{-/-}$ mice (Figure 3C-E). Histological analysis revealed that calcium deposits (von Kossa positive areas) in PCSK9 AAV mice that consumed the HF/HC diet for 20 weeks was similar to those in *Ldlr*$^{-/-}$ mice that consumed the HF/HC diet for 15 and 20 weeks (Figure 3F). Immunohistochemistry localized RUNX2 and osteocalcin — markers of vascular calcification — in the aortic sinus and root of both groups (Supplementary Figure 2A-D).

We further assessed the levels of blood markers of calcification. Plasma phosphate levels increased in PCSK9 AAV mice and *Ldlr*$^{-/-}$ mice, while calcium levels did not change (Supplementary Figure 3A, B). Osteoprotegerin (OPG) levels increased 3-fold in mice that received a single PCSK9 AAV injection and the HF/HC diet for 20 weeks, which were similar to *Ldlr*$^{-/-}$ mice that consumed a HF/HC diet for 15 weeks (Supplementary Figure 3C). Dickkopf-1 (DKK1) decreased in PCSK9 AAV mice and *Ldlr*$^{-/-}$ mice over time (Supplementary Figure 3D).

Mutant mPCSK9 (D377Y) AAV promotes plaque collagen maturation in C57BL/6J mice

In the aortic sinus of wild-type C57BL/6J mice that received a single PCSK9 AAV injection and the HF/HC diet for 15 weeks, fibrillar collagen occupied 70.6 ± 10.5 % of the plaques

that contained 95.5±1.9% mature or thick collagen and 4.5 ± 1.9 % immature or thin collagen (Picrosirius red stain) (Figure 4A-C). The plaque collagen content in the aortic sinus of mPCSK9 (D377Y) AAV mice on the HF/HC diet for 20 weeks was 62.3 ± 3.4 % and composed of 90.6 ± 4.2 % mature and 9.4 ± 4.2 % immature collagen (Figure 4A-C).

Mice that received a single PCSK9 AAV injection and the HF/HC diet for 15 weeks had 31.9±6.6 % collagen area per plaque at the lesser curvature of the aortic arch that contained 84.3 ± 5.9 % mature and 15.7 ± 5.9 % immature collagen (Figure 4D-F). The aortic arch plaque collagen content of PCSK9 mice on the HF/HC diet for 20 weeks increased to 56.1 ± 9.4 % ($p < 0.05$) (Figure 4D-F). Mature collagen increased to 93.4 ± 5.1 % and immature collagen decreased to 6.6 ± 5.1% ($p < 0.05$) (Figure 4D-F). The plaque collagen maturation of PCSK9 AAV mice was similar to those of *Ldlr*$^{-/-}$ mice.

Mutant mPCSK9 (D377Y) AAV induces macrophage accumulation in atherosclerotic lesions in C57BL/6J mice

Lesions of PCSK9 AAV mice and *Ldlr*$^{-/-}$ mice that consumed a HF/HC diet for 15 weeks showed CD68-positive macrophages in the aortic sinus (Figure 4G). *Ldlr*$^{-/-}$ mice on the HF/HC diet for 15 weeks exhibited more advanced aortic arch lesions compared to PCSK9 AAV mice with greater macrophage accumulation in the plaques that appears to have diminished as calcification progresses at the 20 week time point (Figure 4G).

Sortilin-deficiency reduces vascular calcification in the PCSK9 AAV model

We recently reported that sortilin-deficiency in the *Ldlr*$^{-/-}$ background reduces vascular calcification [9]. To demonstrate the usefulness of the PCSK9 AAV model in validating potential therapeutic targets *in vivo*, we injected gain-of-function mutant PCSK9 AAV into sortilin-deficient mice and corresponding C57Bl/6J littermate controls. Both strains express *Ldlr*. All mice were fed the HF/HC diet for 20 weeks. PCSK9 AAV induced sortilin protein expression in atherosclerotic lesions of the C57Bl/6J *Sort*$^{+/+}$ controls (Figure 5A). Vascular calcification induced by a single injection of AAV-encoding mutant PCSK9 decreased in *Sort*$^{-/-}$ mice (−46.9 %, $p < 0.05$) (Figure 5B), while PCSK9 and total cholesterol plasma levels did not change (Figure 5C, D). These data support our previous report [9] and demonstrate the feasibility of the use of this model as an alternative to breeding transgenic mice with *Ldlr*-deficient mice to generate vascular calcification.

Discussion

This study demonstrates that a mouse model of vascular calcification involving a single injection of AAV that encodes for a gain-of-function form of murine PCSK9 (D377Y) and the HF/HC diet in C57BL/6J mice does not require genetic modification. This methodology can speed discoveries in vascular calcification by avoiding time consuming, labor intensive, and costly crossing of a genetically-modified mouse strain with *Ldlr*$^{-/-}$ or *Apoe*$^{-/-}$ mice, a strain susceptible to atherosclerosis.

Previous studies showed that the AAV-mediated long-term gain-of-function of PCSK9 in C57BL/6J and C57BL/6NTac mice provides a powerful model of atherosclerosis [10, 11]. It was suggested that this approach will facilitate studies that use strains of different genetic

backgrounds to search for genes that modify atherosclerotic lesion formation [7]; however, AAV-hPCSK9 mutant injection into 129/SvPas/NCrl and FVB/NCrl mice did not promote atherosclerotic lesion development even though these animals exhibited increased cholesterol levels [11].

Here we show the time course of vascular calcification development in the PCSK9 AAV model. Within the time frame of 15 weeks to 20 weeks, we observed acceleration of vascular calcification. The observed rapid growth is consistent with our recent study on calcification growth that revealed significant change in calcification size and morphology over the course of 3 weeks in *Apoe*$^{-/-}$ mice [17], which are similar to the *Ldlr*$^{-/-}$ mice used in the present study.

The extent of plaque development and vascular calcification induced by 10^{11} virus particles of AAV-PCSK9 was slower than of the same measures in *Ldlr*$^{-/-}$ mice on the same diet. Despite the reduced rate, however, the stages of progression were similar. We noticed that 10-week-old C57/Bl6J mice on a chow-diet had 3-fold less cholesterol levels compared to *Ldlr*$^{-/-}$ mice. This difference may explain the observed 'lag' phase of plaque calcification that is part of the later continuum of plaque development. The increased time required to achieve similar endpoints remains far less than the time required for genetic crossings to produce compound mutant mice with the Ldlr$^{-/-}$ genetic background. Previously reported studies show that a single injection of $3x10^{10}$ AAV-PCSK9 into wild-type C57BL6/J mice induced the similar lesion size to that in *Apoe*$^{-/-}$ mice on the same atherogenic diet [11]. A single injection of 1 or $5x10^{11}$ AAV-PCSK9 into C57BL/6NTac mice caused less lesion formation compared to *Ldlr*$^{-/-}$ mice on a high fat diet. When both groups consumed the HF/HC diet, however, lesion size was similar [10]. This finding is in line with our observation of the similar lesion size in our AAV-PCSK9 and *Ldlr*$^{-/-}$ groups.

AAV-control-injected mice on high-fat diet and AAV-PCSK9-injected mice on a chow diet do not develop atherosclerotic plaques spontaneously [11]. Saline injected mice that consumed the HF/HC diet were used as control and did not display obvious atherosclerotic lesion formation. The data presented here show that a single injection of AAV encoding gain-of-function mutant mPCSK9 (D377Y) is sufficient to induce vascular calcification similar to that in *Ldlr*$^{-/-}$ and *Apoe*$^{-/-}$ mice, commonly utilized strains in atherosclerosis research. We demonstrated the value of the PCSK9 AAV model by demonstrating a reduction of vascular calcification in sortilin-deficient mice, which is consistent with our previous data on the sortilin compound mutant mice with the *Ldlr*-deficient background [9]. Utilizing this method will enhance the efficiency of testing potential modulators of calcification *in vivo* without crossing mice to introduce susceptibility to atherosclerosis. This may help expedite the clinical translation of basic science discoveries of therapeutic targets for cardiovascular calcification, a condition with no medical treatment options.

Supplementary Material

Refer to Web version on PubMed Central for supplementary material.

Acknowledgments

The authors thank Dr. Hengmin Zhang for the injection of AAV.

Source of funding and disclosures of financial support

This study was supported by a research grant from Kowa Company, Ltd. (M.A.). E.A. laboratory is supported by the National Institutes of Health grants R01HL114805 and R01HL109506). M.A. laboratory is supported by the National Institutes of Health grants R01HL107550 and R01HL126901. M.K. laboratory is supported by the Danish Diabetes Academy, Novo Nordisk Foundation.

References

1. Criqui MH, Denenberg JO, Ix JH, McClelland RL, Wassel CL, Rifkin DE, et al. Calcium Density of Coronary Artery Plaque and Risk of Incident Cardiovascular Events. JAMA : the journal of the American Medical Association. 2013 Epub 2013/11/20. PubMed PMID: 24247483.
2. Hutcheson JD, Goettsch C, Rogers MA, Aikawa E. Revisiting cardiovascular calcification: A multifaceted disease requiring a multidisciplinary approach. Semin Cell Dev Biol. 2015; 46:68–77. PubMed PMID: 26358815. [PubMed: 26358815]
3. Martin SS, Blaha MJ, Blankstein R, Agatston AS, Rivera JJ, Virani SS, et al. Dyslipidemia, Coronary Artery Calcium, and Incident Atherosclerotic Cardiovascular Disease: Implications for Statin Therapy from the Multi-Ethnic Study of Atherosclerosis. Circulation. 2013 Epub 2013/10/22. PubMed PMID: 24141324.
4. Joshi NV, Vesey AT, Williams MC, Shah AS, Calvert PA, Craighead FH, et al. F-fluoride positron emission tomography for identification of ruptured and high-risk coronary atherosclerotic plaques: a prospective clinical trial. Lancet. 2013 Epub 2013/11/15. PubMed PMID: 24224999.
5. Vengrenyuk Y, Carlier S, Xanthos S, Cardoso L, Ganatos P, Virmani R, et al. A hypothesis for vulnerable plaque rupture due to stress-induced debonding around cellular microcalcifications in thin fibrous caps. Proceedings of the National Academy of Sciences of the United States of America. 2006; 103(40):14678–14683. Epub 2006/09/28. PubMed PMID: 17003118; PubMed Central PMCID: PMC1595411. [PubMed: 17003118]
6. Kelly-Arnold A, Maldonado N, Laudier D, Aikawa E, Cardoso L, Weinbaum S. Revised microcalcification hypothesis for fibrous cap rupture in human coronary arteries. Proceedings of the National Academy of Sciences of the United States of America. 2013; 110(26):10741–10746. Epub 2013/06/05. PubMed PMID: 23733926; PubMed Central PMCID: PMC3696743. [PubMed: 23733926]
7. Daugherty A, Tabas I, Rader DJ. Accelerating the pace of atherosclerosis research. Arterioscler Thromb Vasc Biol. 2015; 35(1):11–12. PubMed PMID: 25520521. [PubMed: 25520521]
8. Aikawa E, Nahrendorf M, Figueiredo JL, Swirski FK, Shtatland T, Kohler RH, et al. Osteogenesis associates with inflammation in early-stage atherosclerosis evaluated by molecular imaging in vivo. Circulation. 2007; 116(24):2841–2850. PubMed PMID: 18040026. [PubMed: 18040026]
9. Goettsch C, Hutcheson JD, Aikawa M, Iwata H, Pham T, Nykjaer A, et al. Sortilin mediates vascular calcification via its recruitment into extracellular vesicles. J Clin Invest. 2016; 126(4):1323–1336. PubMed PMID: 26950419; PubMed Central PMCID: PMCPMC4811143. [PubMed: 26950419]
10. Bjorklund MM, Hollensen AK, Hagensen MK, Dagnaes-Hansen F, Christoffersen C, Mikkelsen JG, et al. Induction of atherosclerosis in mice and hamsters without germline genetic engineering. Circ Res. 2014; 114(11):1684–1689. PubMed PMID: 24677271. [PubMed: 24677271]
11. Roche-Molina M, Sanz-Rosa D, Cruz FM, Garcia-Prieto J, Lopez S, Abia R, et al. Induction of sustained hypercholesterolemia by single adeno-associated virus-mediated gene transfer of mutant hPCSK9. Arterioscler Thromb Vasc Biol. 2015; 35(1):50–59. PubMed PMID: 25341796. [PubMed: 25341796]
12. Awan Z, Denis M, Bailey D, Giaid A, Prat A, Goltzman D, et al. The LDLR deficient mouse as a model for aortic calcification and quantification by micro-computed tomography. Atherosclerosis. 2011; 219(2):455–462. PubMed PMID: 22051553. [PubMed: 22051553]

13. Al-Mashhadi RH, Bjorklund MM, Mortensen MB, Christoffersen C, Larsen T, Falk E, et al. Diabetes with poor glycaemic control does not promote atherosclerosis in genetically modified hypercholesterolaemic minipigs. Diabetologia. 2015; 58(8):1926–1936. PubMed PMID: 26026653. [PubMed: 26026653]

14. Al-Mashhadi RH, Sorensen CB, Kragh PM, Christoffersen C, Mortensen MB, Tolbod LP, et al. Familial hypercholesterolemia and atherosclerosis in cloned minipigs created by DNA transposition of a human PCSK9 gain-of-function mutant. Sci Transl Med. 2013; 5(166):166ra1. PubMed PMID: 23283366.

15. Huijgen R, Boekholdt SM, Arsenault BJ, Bao W, Davaine JM, Tabet F, et al. Plasma PCSK9 levels and clinical outcomes in the TNT (Treating to New Targets) trial: a nested case-control study. J Am Coll Cardiol. 2012; 59(20):1778–1784. PubMed PMID: 22575316. [PubMed: 22575316]

16. Aikawa E, Whittaker P, Farber M, Mendelson K, Padera RF, Aikawa M, et al. Human semilunar cardiac valve remodeling by activated cells from fetus to adult: implications for postnatal adaptation, pathology, and tissue engineering. Circulation. 2006; 113(10):1344–1352. PubMed PMID: 16534030. [PubMed: 16534030]

17. Hutcheson JD, Goettsch C, Bertazzo S, Maldonado N, Ruiz JL, Goh W, et al. Genesis and growth of extracellular-vesicle-derived microcalcification in atherosclerotic plaques. Nat Mater. 2016 PubMed PMID: 26752654.

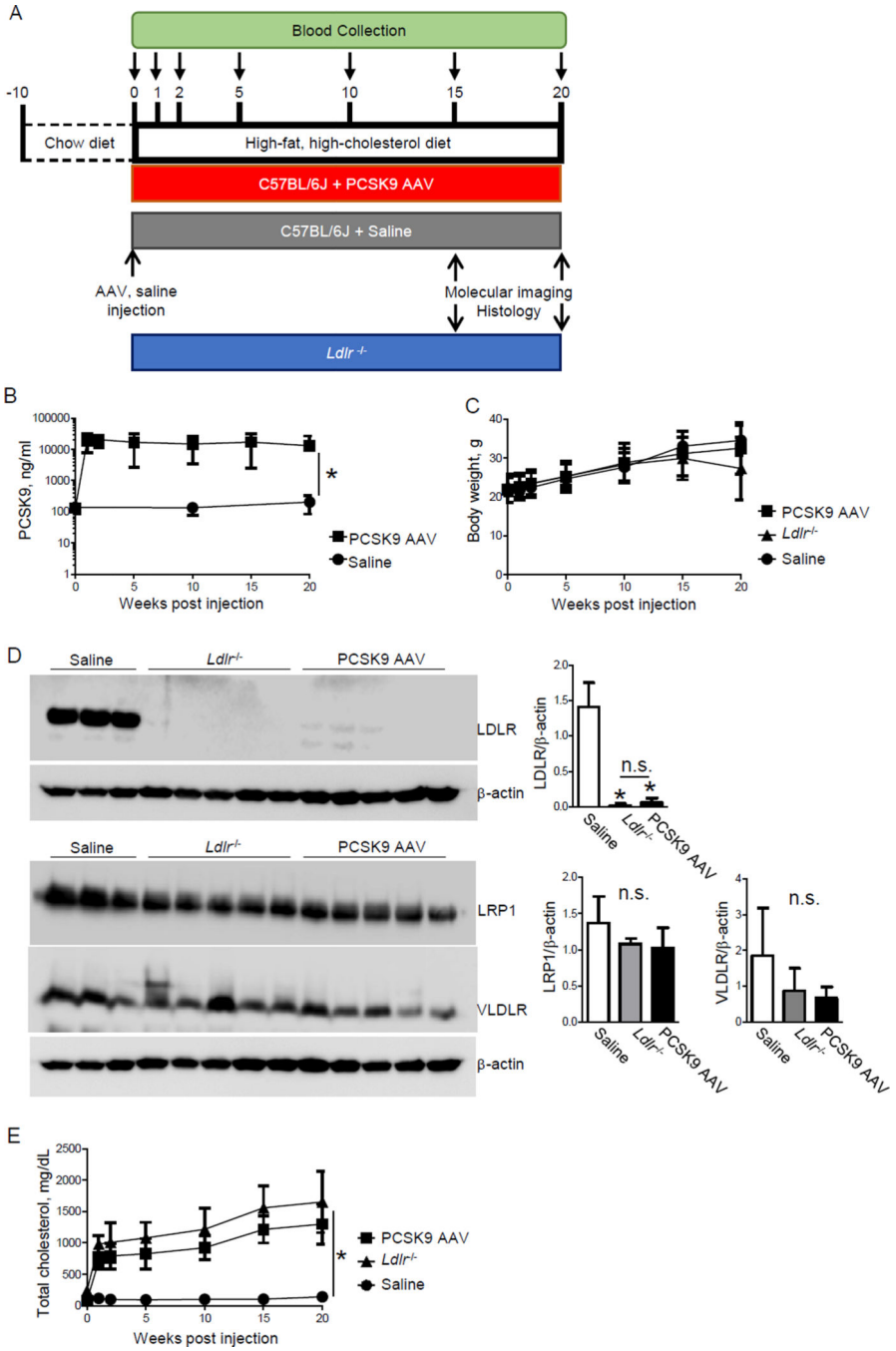

Figure 1. Single injection of AAV-mPCSK9 mutant (D377Y) induces hypercholesterolemia in high-fat, high-cholesterol fed C57BL/6J mice

A) Study design. **B)** Plasma PCSK9 level and **C)** Body weight before injection and at 1, 2, 5, 10, 15 and 20 weeks after injection. **D)** Hepatic LDLR, LRP1 and VLDLR protein expression. β-actin served as loading control. **E)** Plasma total cholesterol levels before injection and at 1, 2, 5, 10, 15 and 20 weeks after injection. *$p < 0.05$ by one-way ANOVA. Data presented as mean±SD.

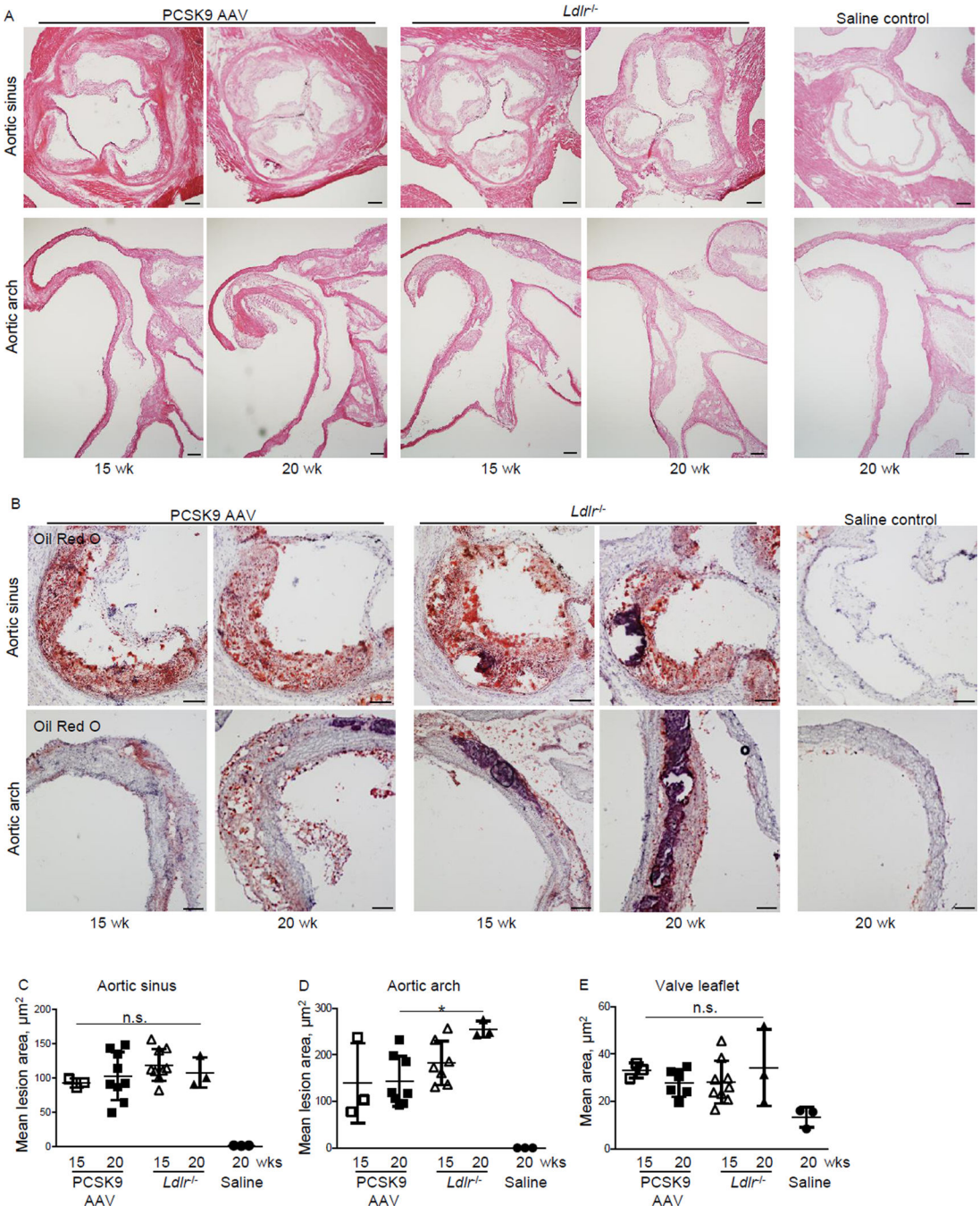

Figure 2. Single injection of AAV-mPCSK9 mutant (D377Y) induces atherosclerotic lesion formation in high-fat, high-cholesterol fed C57BL/6J mice

A) H&E staining of aortic sinus and aortic arch of AAV-mPCSK9- or saline-injected C57BL/6J mice and *Ldlr*$^{-/-}$ mice that consumed a high-fat, high-cholesterol diet for 15 or 20 weeks. Bar: 200µm. **B)** Representative photomicrographs of aortic sinus (top) and aortic arch (bottom) atherosclerotic plaques after Oil Red O staining. Bar: 100µm **C)** Quantification of aortic sinus lesion area. **D)** Quantification of aortic arch (lesser curvature)

lesion area. **E)** Quantification of valve leaflet area. *$p < 0.05$ by one-way ANOVA. n.s., not significant. Data presented as mean±SD. Each dot depicts one mouse. n=3–8 for all panels.

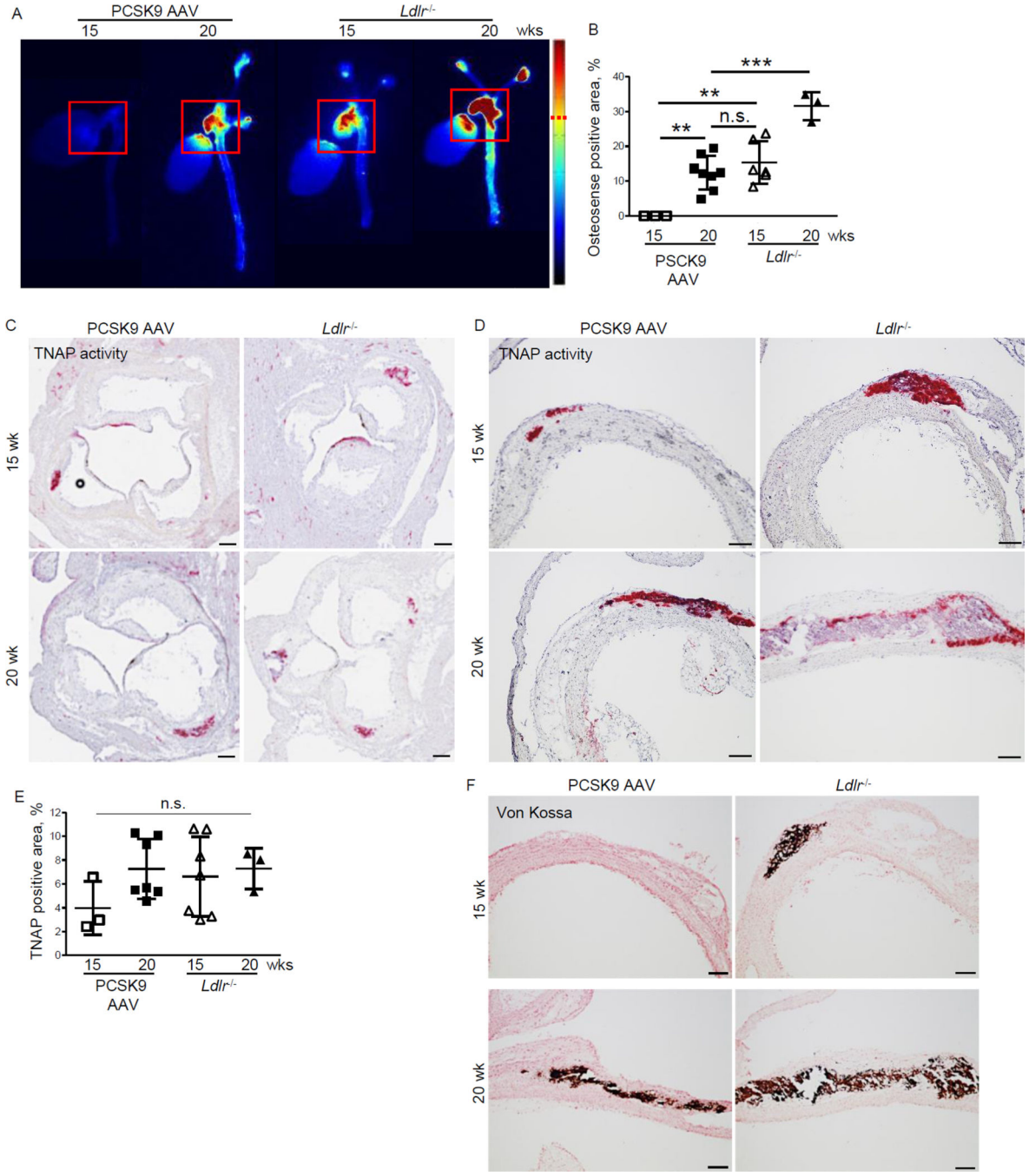

Figure 3. Single injection of AAV-mPCSK9 mutant (D377Y) induces vascular calcification in high-fat, high-cholesterol fed C57BL/6J mice

A) Ex vivo FRI analysis. Representative images of the fluorescence intensity in the aorta. Red squares (200x200 pixel) indicate the quantified area including aortic sinus and arch. **B)** Quantification of FRI signal-positive area (dashed red line indicates signal cut-off for quantification). $^{**}p < 0.01$, $^{***}p < 0.001$ by one-way ANOVA. **C, D)** Representative images of tissue non-specific alkaline phosphatase activity (TNAP stain) in the aortic sinus (C) and aortic arch (lesser curvature) (D). C, Bar=200 μm C; D, Bar=100 μm. **(E)** Quantitative

assessment of %-positive lesion area for TNAP. Data presented as mean±SD. Each dot depicts one mouse. n.s., not significant. **F)** Representative images of von Kossa stain for calcium deposits in the aortic arch (lesser curvature). Bar=100 μm. n=3–8 for all panels.

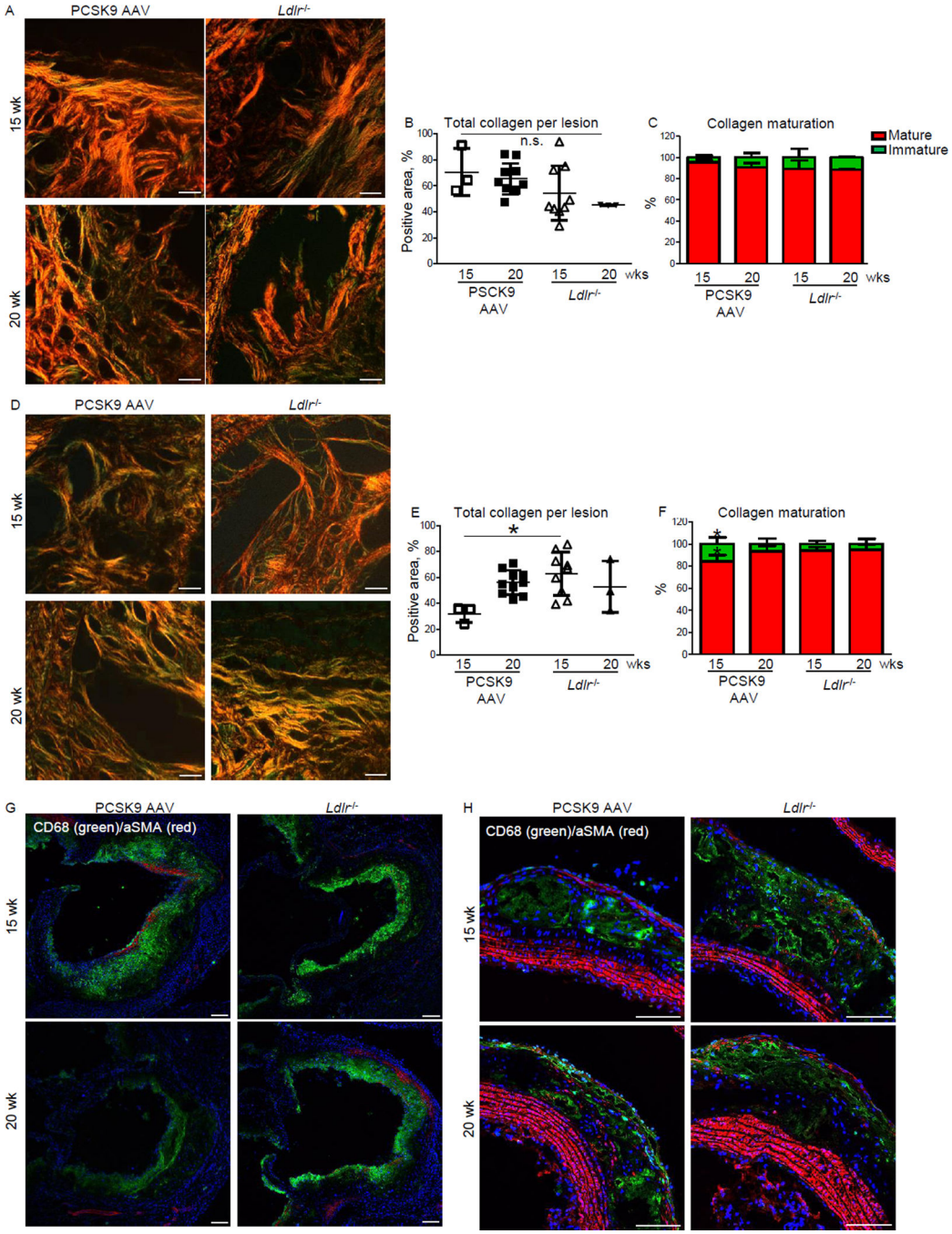

Figure 4. Single injection of AAV-mPCSK9 mutant (D377Y) induces collagen remodeling and macrophage infiltration in high-fat, high-cholesterol fed C57BL/6J mice

A) Representative images of picrosirius red staining for fibrillar collagen in the aortic sinus. Bar=20 μm. **B)** Quantification of total collagen from A. **C)** Quantification of mature/thick (red) and immature/thin (green) collagen (collagen hue analysis) from A. **D)** Representative images of picrosirius red staining of aortic arch (lesser curvature). Bar=20 μm. **E)** Quantification of total collagen from D. **F)** Quantification of mature/thick (red) and immature/thin (green) collagen from D. Data presented as mean±SD. Each dot depicts one

mouse. *$p < 0.05$ by one-way ANOVA compared to all other groups. n=3–8 for all panels. **G, H)** Representative double immunofluorescence staining of CD68 (macrophages, green)/α smooth muscle actin (αSMA, red) in the aortic sinus (G) and aortic arch (H). Bar=100 μm. n=3.

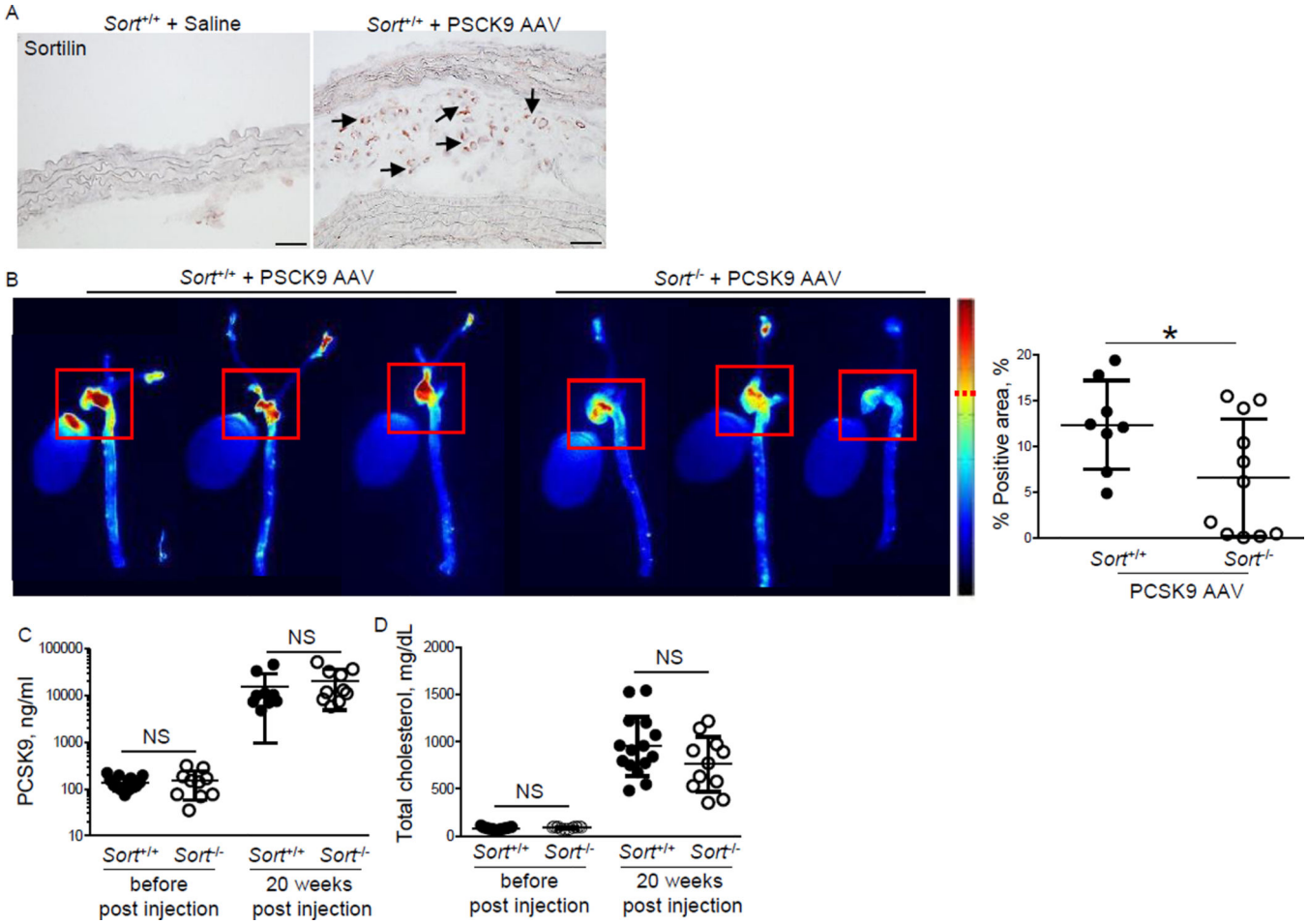

Figure 5. Sortilin-deficiency reduces vascular calcification induced by a single injection of AAV-mPCSK9 mutant (D377Y) in high-fat, high-cholesterol fed C57BL/6J mice

A) Representative images of sortilin immunohistochemistry of saline- and mPCSK9 AAV-injected C57Bl/6J mice (*Sort*$^{+/+}$). Arrows indicate positive immunoreactivity. Bar=50μm. B) Ex vivo FRI analysis. Representative images of the fluorescence intensity in the aorta. Red squares (200x200 pixel) indicate the quantified area including the aortic sinus and arch. Quantification of FRI signal-positive area (dashed red line indicates signal cut-off for quantification). *$p < 0.05$. **C)** PCSK9 plasma levels. **D)** Plasma total cholesterol levels. NS: not significant. Data presented as mean±SD. Each dot depicts one mouse.